PROC. OF JSCE
No. 341, January 1984

FATIGUE STRENGTHS OF TRUSS MADE OF HIGH STRENGTH STEELS

By Jiro TAJIMA, Koei TAKENA**, Chitoshi MIKI*** and Fumio ITO*****

1. INTRODUCTION

The fatigue design criteria for Honshu-Shikoku bridges were established in 1973 by the technical committee in the Japan Society of Civil Engneers[1]. The allowable fatigue stresses were set based on the approximate lower limits (lower 95% tolerance limit) for the available fatigue test results on various welded joints. However, in past fatigue tests, configurations and dimensions of specimens were fairly restricted due to the capacity of fatigue testing machines. Considering the scale of Honshu-Shikoku bridges, it must be further confirmed the appropriateness of these allowable stresses for fatigue. Accordingly, Honshu-Shikoku Bridge Authority has been carrying out the fatigue tests of various types of large-size welded joints and structural models by the use of the fatigue testing machine with the 4 MN loading capacity[2]. Based on the results of these tests, the fatigue design criteria was revised in 1981[3].

The objective of this study is to investigate the fatigue behavior of trusses. Various types of panel-point-structures were designed for the purpose of obtaining compact and strong nodal joint, and fatigue tests of the structural models on the scale of about one quarter were carried out. In previous fatigue tests of panel point structures of trusses by authors et al.[4),5)]. fatigue cracks originated from the end of diaphragm which was inserted between two gusset plates as the continuation of the diagonal members after only a small number of cycles of stress repetition. A large number of fatigue cracks were also observed at the corner weld of bottom chords too. Based on the previous study[4),5)], details of nodal joint were improved and the process of corner weld was changed from manual shielded arc welding to submarged-arc welding. The local stresses distribution in the vicinity of nodal joint and their influences on the fatigue strength are also shown through the finite element stress analysis.

2. SPECIMENS

Fatigue tests were performed using the loading apparatus shown in **Fig. 1**. The dotted portion in this figure represents a specimen. Test specimen is inserted in the loading apparatus by high strength bolt joints. **Fig. 2** shows configurations and dimensions of the specimens. The design procedure for these specimens conformed to the design standard for super structures of Honshu-Shikoku bridges[6]. The mechanical properties of steels are shown in **Table 1**. Three different type of specimen are tested to verify the most appropriate method of connection of the diagonal members to the bottom chord. In type D specimen, diagonal members are connected to bottom chord only by gusset plates. The diaphragm which is set between gusset-plates in type E and H specimen is expected to transmit some part of the axial force of

* Member of JSCE, Dr. of Eng., Professor, Dept. of Construction Engineering, Saitama University.
** Member of JSCE, Engineer, Honshu-Shikoku Bridge Authority
*** Member of JSCE, Associate Professor, Tokyo Institute of Technology
**** Member of JSCE, Research Engineer, Japan Construction Method and Machinery Research Institute.

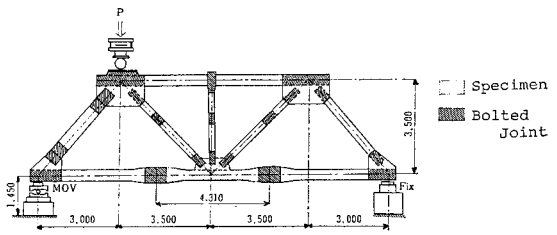

Fig. 1 Loading apparatus.

Table 1 Mechanical propaties of steel used.

Specimen Type	Steel	Yield Point (MPa)	Tensile Strength (MPa)	Elongation (%)
D.E.F.	SM58*	559	647	36
G	HT80**	784	823	31
H	HT80	794	843	30

* 600 MPa class steel
** 800 MPa class steel

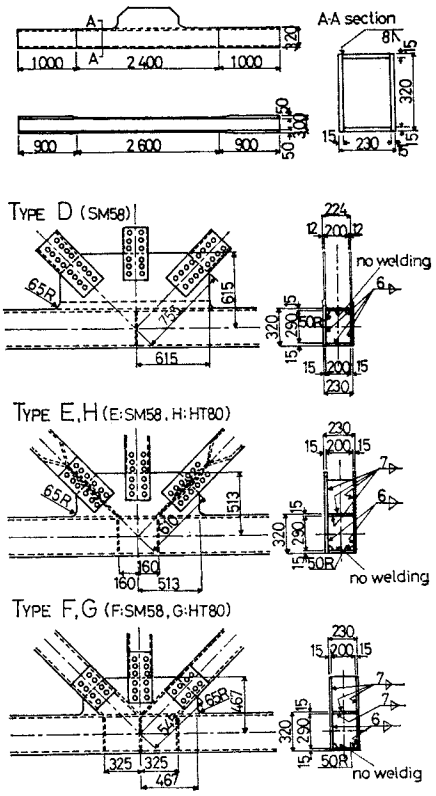

Fig. 2 Configurations and dimensions of the specimens.

diagonal member to the upper flange of bottom chord directly. By the adoption of this diaphragm, the size of gusset-plate become small.

The corner weld of chord members were performed using the submerged-arc process. Due to the unexpected failure of preheating operation, a large number of blowholes occurred in the corner welds of the bottom chord of type D,E,F and G specimens.

3. TEST SET-UP AND TEST PROCEDURE

Fatigue tests were performed with a servo-type fatigue testing machines of maximum

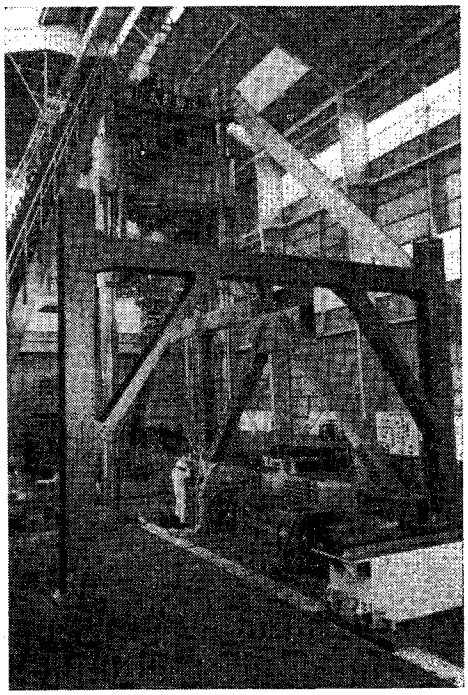

Photo 1 Loading arrangement.

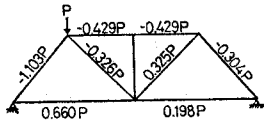

Fig. 3 Axial forces in each member.

dynamic loading capacity of 4 MN. **Photo 1** shows the loading arrangement. A single compressive load is applied on the node at the upper left of the loading apparatus shown in **Fig. 1.** The calculated axial forces in each member when a load P is applied are shown in **Fig. 3.**

Prior to the fatigue tests, static loading tests were conducted. In order to determine the stress distribution within the nodal joint and to find axial stresses and secondary stresses in the chord members, many strain gages were placed on specimens. Strain readings were also measured at certain intervals during the fatigue tests. Furthermore, the stress analysis by the use of finite element method were done and compared to the measured stresses. The analysis was undertaken using the plane stress triangular element. Minimum mesh size was about 10 mm for all types of specimen.

The loading wave form was sinusoidal and loading rate was 2.3 Hz. Visual inspection, dye-penetrant technique and magnaflux inspection

Table 2 Stress in parallel portion of chord.

Specimen	Load (MN)		Max. Stress (MPa)		Stress Range (MPa)	
	Max.	Min.	predicted	measured*	predicted	measured*
D-1	3.7	0.2	153	150	145	142
-2	3.0	0.2	124	118	116	110
E-1	3.0	0.2	124	126	116	112
-2	3.0	0.2	124	126	116	112
F-1	3.0	0.2	124	123	116	115
-2	3.7	0.2	153	149	145	141
G-1	3.0	0.2	124	122	116	114
-2	3.0	0.2	124	120	116	112
H-1	3.0	0.2	124	120	116	112

* Average value of 14 data (in some case 12 data) at 4 points on the surface of webs of bottom chord member (in some cases 2 points) and 3 points on the surface of fianges.

were carried out at preselected intervals to moniter the initiation and growth of fatigue cracks.

4. STRESS DISTRIBUTIONS

Table 2 gives predicted and measured stresses in the parallel portion of bottom chord. These results indicate that the axial forces applied to the specimens actually are almost the same as the predicted values.

Principal stresses in the gussets were calculated from measured strains and plotted in **Fig. 4.** They are compared to the computed principal stresses by the finite element method. Both are in fairly good agreement. Stresses only D-1 specimen in the direction of diagonal members are somewhat higher than those in other type specimens. Overall stress distributions in three type nodal-structures are resemble to each other.

Measured stresses are also compared with predicted stresses along the upper and lower reference lines (line 4 and 5) in **Fig. 5.** Measured stresses generally coincide with predicted stresses.

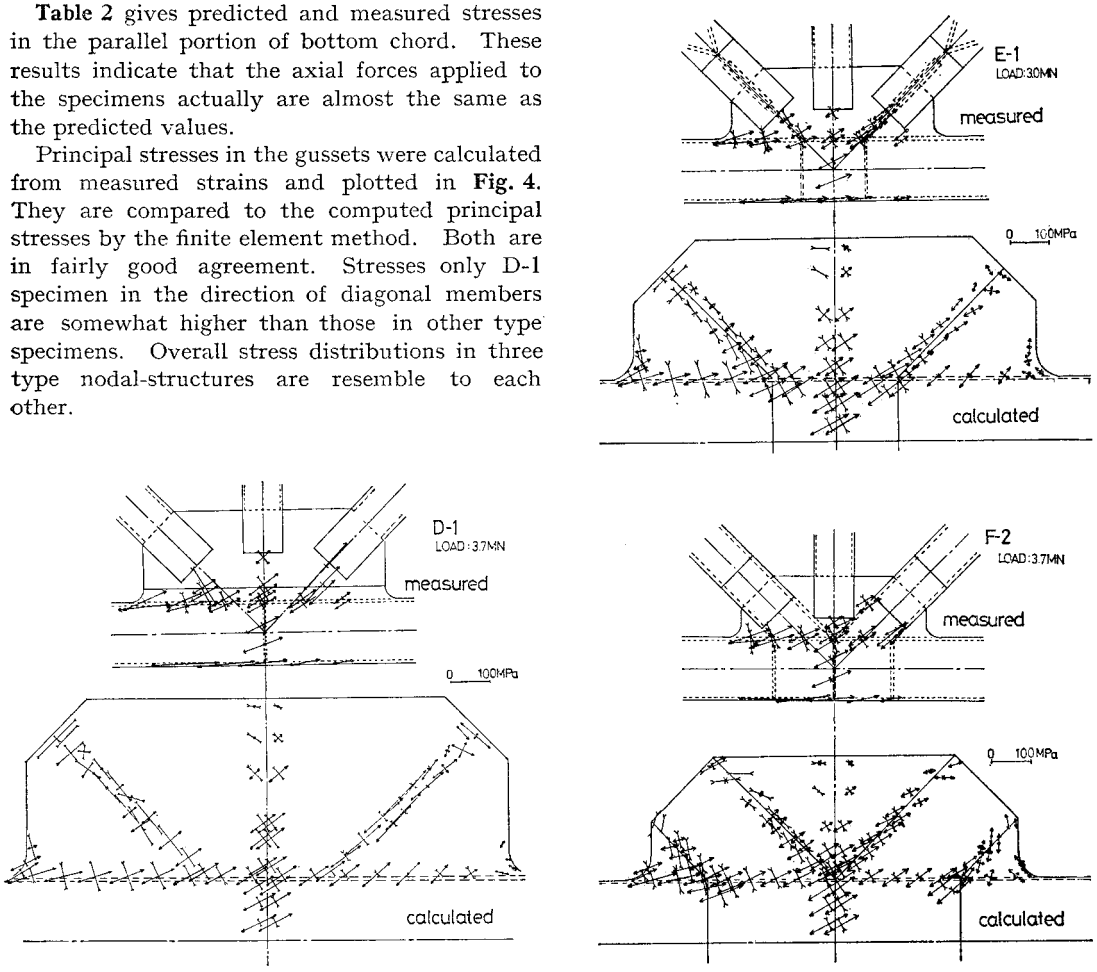

Fig. 4 Distribution of principal stress in nodal joint.

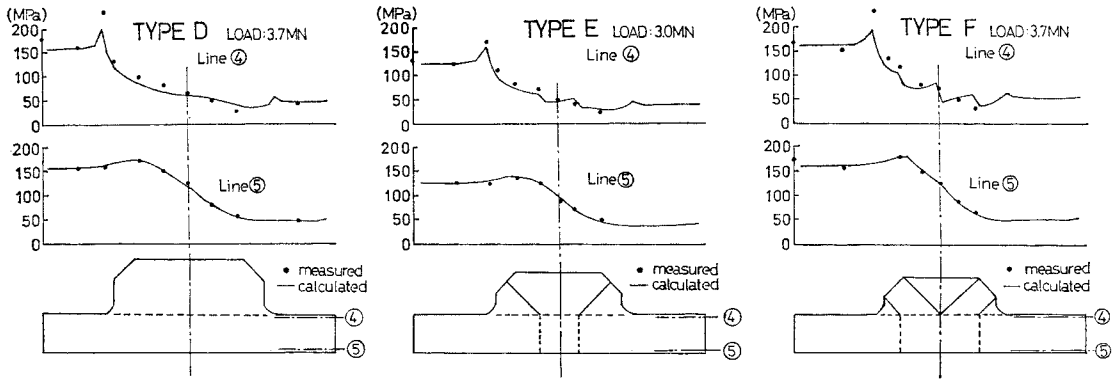

Fig. 5 Stress distribution on the edge lines of lower chord.

Table 3 Stress at the end of fillet.

Specimen Type	Nominal Stress S_0 (MPa)	Stress at the Fillet End		K_t	
		Calculated S_{cal} (MPa)	Measured S_{mea} (MPa)	S_{cal}/S_0	S_{mea}/S_0
D	166	209	239	1.25	1.44
E	166	208	218	1.25	1.31
F	166	203	224	1.22	1.35
G	166	203	226	1.22	1.36
H	166	208	211	1.25	1.27

For the convenience of comparison, all stresses were converted into these under 4 MN.

At the end of the fillet of gusset plate, stress concentration is observed. In **Table 3**, measured and predicted stresses at the end of fillet are shown. The differences between measured and predicted stresses may be mostly caused by the coarse mesh division of the finite element analysis. The ratio (K_t) of maximum stress at the vicinities of fillet to the stress in the parallel portion of chord are 1.25–1.44 from measured values, and 1.22–1.25 from predicted values. In type D specimen, the transmission of the forces between bottom chord and diagonal member is performed through only gusset plates. In other type of specimens, some part of the forces of diagonal members are transmitted directly into the upper flange of bottom chord through the diaphragm which is placed between gusset plates. Consequently, higher stresses are introduced in the gusset plate of type D specimen and the stress concentration ratio (K_t) at the fillet end is higher than those of others.

Along the reference line 5 in **Fig. 5**, stresses inside nodal joint are slightly higher than those on the parallel portion of bottom chord. Stress concentration ratio in this region is about 1.1 and the same degree in all type specimen. Therefore, in the case that diaphragm in the bottom chord is connected with the lower flange of chord by fillet weld, good profile of weld-toe is required in the prevention of fatigue cracking.

Fig. 6 (a) shows the distribution of axial stresses (σ_x) on the surface of gusset plate along the vertical reference line and on the surface of the lower and upper flange of the bottom chord in type E specimen. Computed stress distribution is in good agreement with measured stress distributions. **Fig. 6** (b) shows the distribution of axial stresses (σ_x) and principal stresses (σ_1) along the reference lines a, a', b and b', which are along the diaphragms in the bottom chord and between gusset plates. Axial stresses decrease gradually from the edge of lower flange toward the upper flange. However, decrease of principal stresses is not so remarkable as compared with that of axial stresses. In particular, in the right side of gusset plate where the force of diagonal member is tension, the principal stress at the edge of the upper flange is higher than that at the edge of the lower flange. These stress distribution is due to the shearing stress induced through the gusset plate. In type E, F, G and H specimen, the end of diaphragm between gusset plates is connected with the upper flange of bottom chord by welding. Because this diaphragm is inclined and this is surrounded by gusset plates, it is difficult for a welder to weld in a good welding condition. Since axial stresses in the upper flange are fairly low compared with these in parallel portion as shown

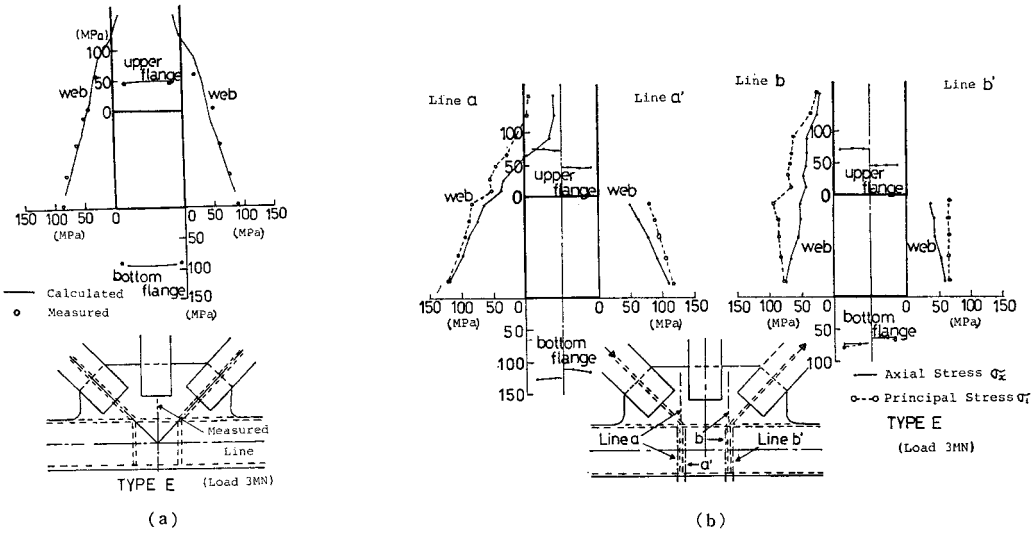

(a) (b)

Fig. 6 Calculated and measured axial stresses σ_x on the panel point section.

Table 4 Results of fatigue tests.

Specimen	Crack No.	Location of Crack	S_r (MPa)	N_c ($\times 10^3$)	l_c (mm)	N_f ($\times 10^3$)	l_f (mm)	Si zeof Blowhole** (mm)	Remarks
D-1	1	UF	152	1405	21		43×33	2.0	Repaired by H.T.B. at n=1465000
	2	LF	154	1420	17	2062	-	-	Repaired by welding
	3	LF	145	1434	6		-	-	〃
	4	LF-Joint	127	1465	12		-	-	〃
	5	LF	145	1465	15		-	-	〃
	6	UF	152	1465	15		-	-	〃
	7	UF-Joint	143	1465	9		-	-	〃
	8	UF-Joint	101	1465	5		55×70	-	Repaired by H.T.R.
	9	LF	145	2025	21		22	2.5	
	10	LF	145	2062	1.5		1.5	-	Observed by MT after the testing
D-2	1	UF-Fillet	165	2365	26	2770	40×30	1.0	Repaired by H.T.B. at n=2365000
	2	LF-Center	88	2747	14		15	3.4	
	3	LF-Center	88	2747	13		16	3.4	From the toe of fillet welds
E-1	1	UF	115	1060	4	1983	5	4.3	Repaired by H.T.B. at n=1983000
	2	UF	115	1850	9		11	5.0	
E-2	1	UFW-Joint	113	1671	7×7	2521	12×12	0.1	Repaired by H.T.B. at n=1671000
	2	UF	113	1728	-		19	3.5	〃 at n=2134000
	3	LF-Gusset	111	1930	12		226×34	3.0	
	4	UF	113	1728	6		×234	4.0	〃 at n=2134000
	5	UF	113	2000	6		18	4.0	〃 〃
	6	UF-Fillet	147	2132	49×38		15	1.5	Crack stopped at the bolt hole
	7	LF-Gusset	123	2135	15		-	3.3	
	8	LF-Gusset	123	2140	10		18	2.8	
	9	UF	116	2140	6		13	2.6	
F-1	1	LF-Gusset	133	2145	17	2582	full sec-	2.0	
	2	UF	114	2158	5		tions 33	2.5	
F-2	1	UF-Fillet	202	1070	6	1583	-	-	Repaired by welding at n=1200000
	2	UF	146	1200	5		-	-	〃 〃
	3	LF-Gusset	163	1200	5		-	-	〃 〃
	4	LF-Gusset	155	1564	41×19		47×30	3.0	
G-1	1	UFW-Joint	112	1673	6×6	2481	20	0.1	Repaired by H.T.B. at n=1673000
	2	LFW-Joint	114	1673	7×8		25	0.1	〃 〃
	3	UF	113	2106	8		70	3.5	
G-2	1	UF-Fillet	157	2293	32×12	2294	32×12	1.8	
H-1	1	W-Joint	102			2000		-	Crack did not appear on the surface
	2	UF	102					1.0	
	3	UF	113			2000		2.4	

* UF: upper flange of bottom chord, LF: lower flange of bottom chord, W: web of bottom chord

** diameter of the inscribed circle in the blowhole

S_r: measured stress range, N_f: final stress cycles, l_f: crack length at N_f

in **Fig. 5**, no fatigue crack occurred from this fillet weld.

5. RESULTS OF FATIGUE TESTS

Results of fatigue tests are summarized in **Table 4** and **Fig. 7**. Observations of fatigue crack were performed at an appropriate interval. In **Table 4**, the number of cycles when the fatigue cracks a detected on the specimen surface (N_c) and the dimension of fatigue crack (l_c) at this cycles are shown. Stress ranges (S_r) in **Table 4** are average stresses measured by strain gages near the fatigue crack initiation point.

Fatigue tests of all specimens were terminated by the growth of fatigue cracks in the bottom chords. The first purpose of this test is to confirm the fatigue strength of various types of panel point structures. Therefore, in order to continue the fatigue test, fatigue cracks which initiated in the corner welding of the chord members at early stage of fatigue tests were repaired by welding or by fastening with the high strength bolts.

After fatigue tests, all portions where fatigue cracks were detected on the surface were cut off from the specimen. These pieces were broken apart to expose the fatigue crack surface. In **Photos 2~5**, some examples of fracture surface are shown. **Photo 2** shows the fracture surface of D-1-1 crack. A blowhole appears on the fracture surface as rounded cavity with a smooth and shiny surface. Twenty-four cracks in thirty-four-cracks were observed by exposure of cracked portion in the eight specimens of the D, E, F and G type specimens. Nineteen fatigue cracks originated from the same kind of blowholes as shown in **Photo 2**.

Photo 3 shows the fracture surface of D-2-1 crack. This crack appeared at the end of the fillet of gusset. The size of the blowhole on this fracture surface is considerably small as compared with others in the parallel portion of bottom chord. The location of this cracking coincides with the point of stress concentration caused by the gusset plate as shown in **Fig. 5**. Due to the high intensity stress, the fatigue crack originated from this small blowhole. In order to continue the fatigue test, this crack was repaired with splice plate fastened with high strength bolts. By the stress repetition after this repairing, this fatigue crack penetrated into bolt-holes. In E-2 and G-2

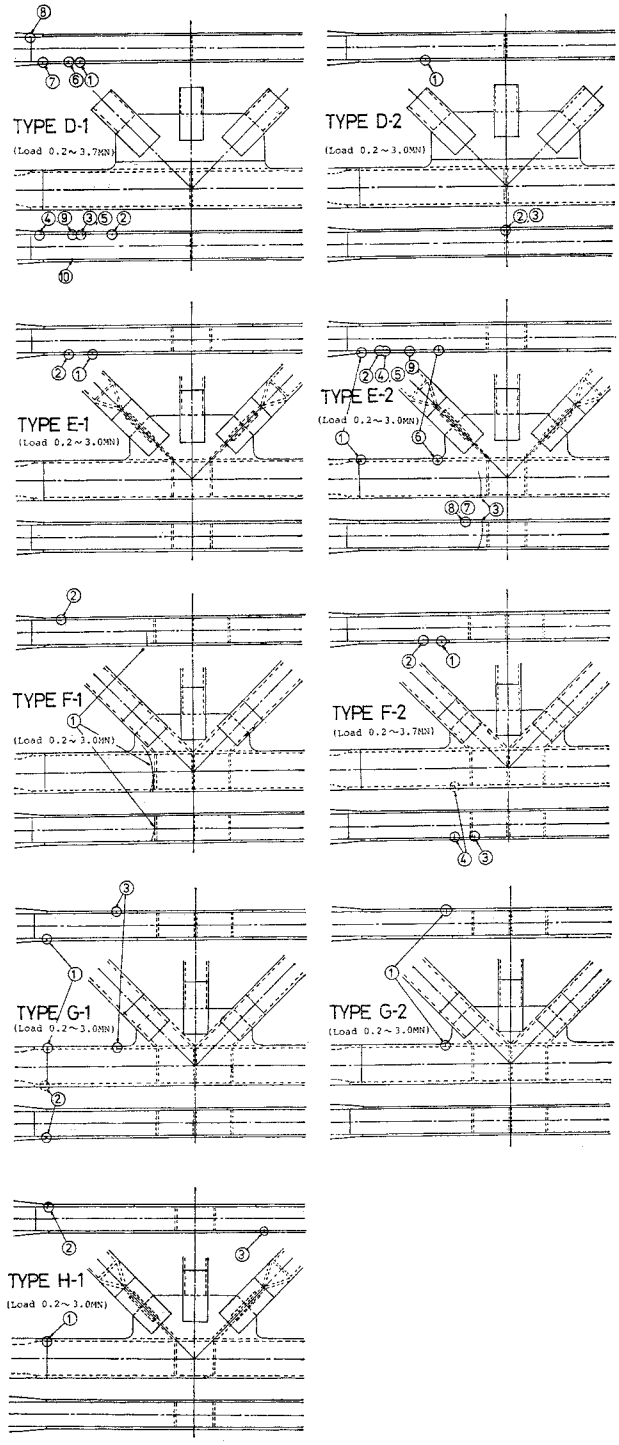

Fig. 7 Results of fatigue tests.

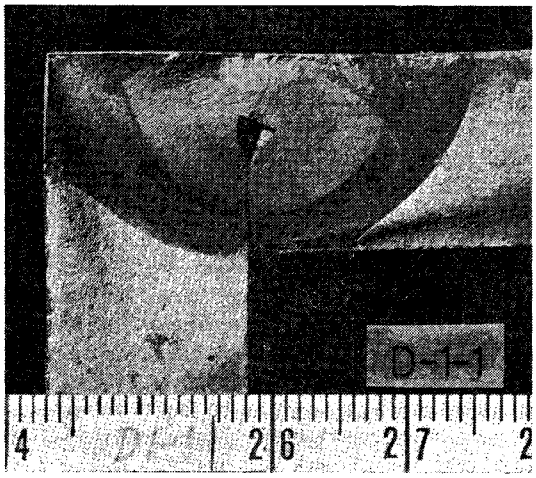

Photo 2 Fracture surface of D-1-1.

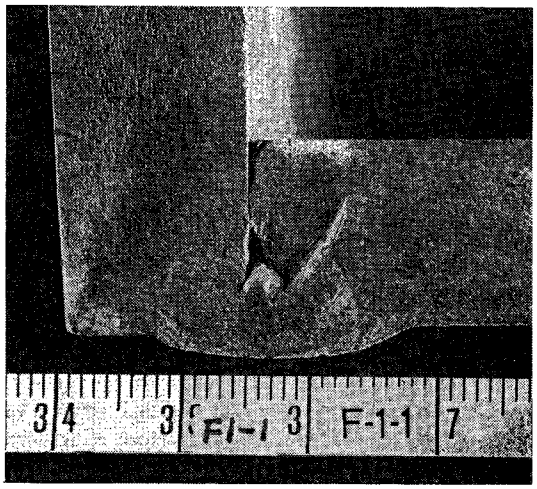

Photo 5 Fracture surface of F-1-1.

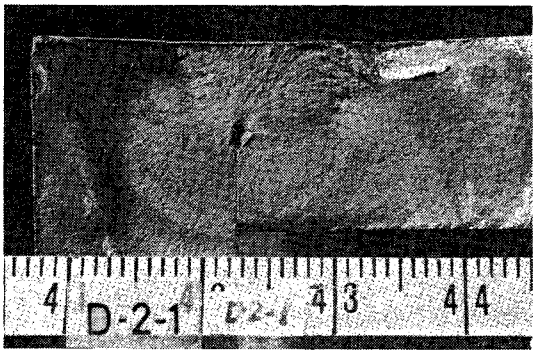

Photo 3 Fracture surface of D-2-1.

specimens, fatigue cracks also appeared at the end of gusset plate. These fatigue cracks originated from the blowholes of same size as that in D-2-1 crack. In D-2 specimen, one fatigue crack originated at the weld-toe of diaphram (D-2-3 Crack).

Photo 4 shows E-2-1 fatigue crack. This crack originated at the corner of the web plate of bottom chord. This cracking is in the butt weld to join the 15 mm web plate and 45 mm web plate. By the observation of fracture surface through a scanning electron microscope, many pipe-like small blowholes were detected at the starting point of fatigue crack. Normally high tensile residual stresses by corner weld is supposed to exist at this place. The fatigue crack started from this very small blowholes may be attributed to the effects of multiple flows and the high tensile residual stress. The same type of cracks are also observed in G-1 specimen (G-1-1 and G-1-2 crack).

Photo 5 shows F-1-1 fatigue crack. This crack initiated very close to the diaphragm in the nodal joint. However, exposed fracture surface indicates that this crack started from a blowhole

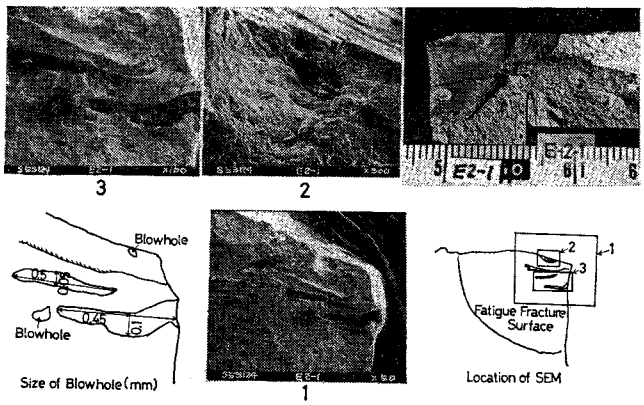

Photo 4 Fracture surface of E-2-1.

in the corner weld. As shown in **Fig. 5**, stress in this region is slightly higher than that in parallel portion.

In H-1 specimen, no fatigue crack was observed until 2×10^6 cycles of loading. The fatigue test of this specimen was continued after specimen-side was changed, this is fixed side was moved to movable side. The fatigue test was continued to more 2×10^6 cycles. However, no fatigue crack was observed on the surface of specimen by this additional stress repetition. During the latter half of the test, fatigue test was performed under two-stage multi-stress range in order to leave beach marks on the fatigue fracture surface. Stress histories are shown in **Fig. 8**. After the fatigue test, all corner welds of bottom chord are broken apart along their respective weld line to observe the penetration of weld metal, blowholes and fatigue cracks. By this observation, two fatigue cracks from blowholes H-1-2 and H-1-3 cracks) and many linked small cracks (H-1-1 crack) in the region of the butt weld of web-plate are observed. H-1-2 and H-1-3 cracks are exposed by the rupture of cracking regions perpendicular to the welding line. The fatigue crack H-1-2 shown in **Photo 6** started from a blowhole and two beach marks were left on the fracture surface. Stress range at this portion during the latter half of the test was 35 MPa. Therefore, this fatigue crack grew under the relatively small stress range. H-1-3 fatigue crack shown in (**Photo 7**) originated also from a blowhole. This specimen was subjected to stress range reduction to one half seven times, from which seven beach marks are observed on the fracture surface. Therefore, it is clear that first beach mark was formed by the first halving of the stress range, and this fatigue crack originated at the early stage after the change of specimen-side.

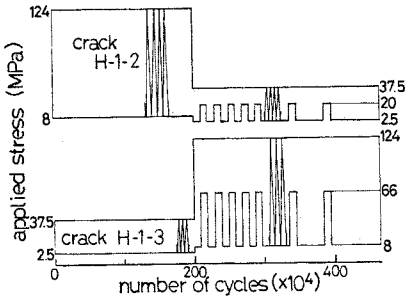

Fig. 8 Stress histories of H-1 specimen.

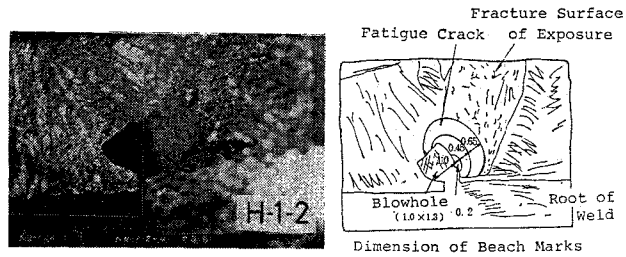

Photo 6 Fracture surface of H-1-2.

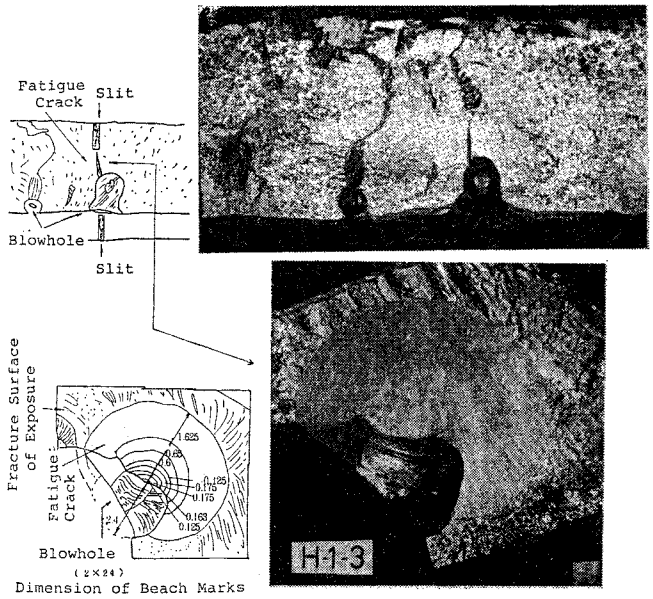

Photo 7 Fracture surface of H-1-3.

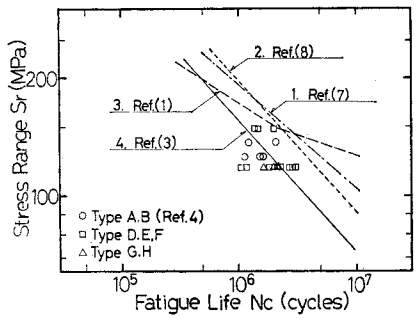

Fig. 9 Results of fatigue tests

6. FATIGUE STRENGTHS OF CHORD-MEMBER

Fig. 9 shows the relations between nominal stress range (S_r) calculated in the parallel portion of bottom chord and N_c. The lower 95% tolerance limit of the longitudinal welded joint at 2×10^6 cycles, which is obtained from the results of past fatigue tests on small scale specimens, is 220 MPa[6]. Fatigue strengths of the corner welds in this study are lower than this value. In **Fig. 9**, dashed-dotted line (line-1) is the mean life of fatigue test results of longitudinal welded joints containing large blowholes in previous study[7]. The size of blowholes in these specimens are 1.80 ×4.20 mm to 3.75×5.30 mm (width×length). The dotted line (line-2) represents the test results of plain welded beams by Hirt and Fisher[8]. This line results from a least squares fit to the test data for beams failing from porosity in longitudinal fillet weld. Porosity of these beam seem to be similar defect to blowhole obtained in this study. However, fatigue strength of bottom chords in this study are low as compared with the previous test results. Dashed line (line-3) is the previous design allowable stress[1] of Honshu-Shikoku Bridges for this joint under pulsating stress. All test results here are below this line. Solid line (line-4) represents the current design allowable stress[3] range of the current fatigue design code of Honshu-Shikoku Bridges. Approximately 50 percent of the test results are still below this line.

Because the greater part of the fatigue life of the partially penetrated corner joint is spent in the growth of fatigue crack,[9),10)] the prediction of fatigue crack growth life using the fracture mechanics concepts is appretiate. Fatigue crack growth life of corner welds when a fatigue crack originates from a root blowhole is predicted based on the following assumptions.

(i) A fatigue crack originates from a defect at the center of plate. The initial defect is regarded as a penny-shaped crack. This shape is maintained through the fatigue crack growth. Stress intensity factor range (ΔK) for this crack can be described as follows.

$$\Delta K = S_r\sqrt{\pi a}\,\frac{2}{\pi}\sqrt{\sec\left(\frac{\pi a}{t}\right)} \quad \cdots\cdots\cdots\cdots (1)$$

S_r: stress range
a: radius of crack
t: plate thickness

(ii) The initial crack radius a_1 is assumed to be equal to the radius of the inscribed-circle in the blowhole[7].

(iii) The final crack size (a_f) is supposed to be 90% of the distance from the root of corner welds to the surface of plate.

(iv) Eq. (2) represent the relation of stress intensity factor range (ΔK) and crack growth rate (da/dN). This relation is the result of fatigue crack growth tests of center-cracked-type specimens containing tensile residual stress.[10]

$$da/dN = 5.47\times10^{-12}((\Delta K)^3-(2.5)^3) \quad \cdots\cdots (2)$$

da/dN: m/cycle
ΔK: MPa$\sqrt{m}$

Fig. 10 shows predicted relations between stress range (S_r) and fatigue crack growth life (N_p) of the bottom chord of truss. The initial crack size a_i is assumed as 0.5, 1.0, 1.5 and 2.5 mm. Test results are classified and plotted in accordance with the radius of the inscribed circles of root blowhole R_i measured on fracture surface (See **Table 4**). The stress range is the measured stress shown in **Table 4**.

Three fatigue cracks initiated at the fillet-end of the gusset plate were classified into $R_i<1.0$. The test results are located close to the predicted S_r–N_p curve of $a_i=0.5$ mm. All test results which classified $1.0\leqq R_i<1.5$ lie beyond the predicted S_r–N_p curve of $a_i=1.5$ mm toward the longer life-side. Consequently, the replacement of root blowhole to the crack of inscribed circle size does

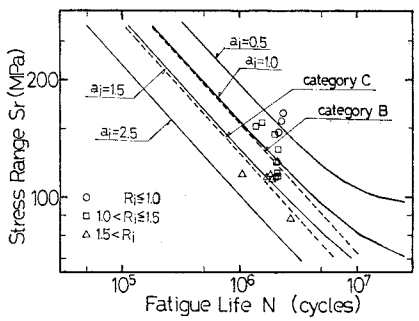

Fig. 10 Predicted S_r–N_p relations and test results.

not give risk-side predicted results and is an apt approximation.

In **Fig. 10**, the current design allowable stress curves for Category B and C joints are shown for comparison. The design curve for Category B agree well with the predicted S_r–N_p curve of $a_i=1.0$ mm. The design curve for Category C is close to the predicted S_r–N_p curve of $a_i=1.5$ mm. For the design of corner welds, the design curve for Category B is employed, therefore weld defects as blowholes exceeding 1.0 mm in the radius of inscribed circle must not be contained in corner welds.

At the fillet end of gusset plate, stresses are higher than those in the parallel portion of the bottom chord, and fatigue cracks originate from smaller blowholes. Therefore, it is recommendable that fatigue design curve for Category C should be applied to corner welds adjacemt to the fillet end of gusset plate. If it is assumed that blowholes of a size exceeding 0.5 mm in the radius of inscribed circle are excluded in this portion, allowable stress for Category B is applicable.

7. SAMMARY OF FINDINGS

The main findings of this study are as follows.

(i) All fatigue tests were terminated by the growth of fatigue cracks initiated in the corner welds of bottom chord members. Most of fatigue cracks originated from blowholes at the weld root of corner weld.

(ii) In the case that blowholes of large size are contained in corner welds, fatigue failures occurred under fairly low stresses which are below the allowable stress for Category B joints.

(iii) Predicted S_r-N_p curve for corner welds containing root blowholes by the application of fracture mechanics concept are close to the experimental results. The design allowable stress curve for Category B almost coincide with the predicted S_r–N_p curve of $a_i=1.0$ mm. Therefore, weld defects as blowholes exceeding the radius of inscribed circle of 1.0 mm must not be contained in the root of corner welds, when Category B curve is employed for corner weld.

(iv) At the fillet end of gusset plate, fatigue cracks originated from the small blowholes due to the stress concentration by the gusset-plate. The size of these blowholes are considerably small as compared with others in the parallel portion of bottom chord. Category C design condition should be applied for this portion. If blowholes exceeding 0.5 mm in the radius of inscribed circle can be excluded, Catogory B is applicable.

(v) Some fatigue cracks initiated from small pipe-like blowholes at the corner of the butt-weld of the web plate of bottom chords. These fatigue cracking may be attributed to the effects of mutiple flows and the high tensile residual stress.

8. ACKNOWLEDGEMENTS

The experimental work was done by researcher Y. Eguchi, H. Takenouchi and S. Tanifuji of the Japan Construction Method and Machinery Research Institute, and stress calculation by finite element method was done by T. Nogawa, former student of Saitama University. The preparation of the paper was done aided greatly by research associate T. Mori of Tokyo Institute of Technology and K. Yamada, technical assistant of Saitama University. The authors wish to express their sincerest gratitute to all those mentioned above.

REFERENCES

1) Japan Society of Civil Engineers, Committee for Honshu-Shikoku Bridges: Fatigue Design for Honshu-Shikoku Bridges. 1974 (In Japanese).
2) Tajima, J., T. Asama, C. Miki and H. Takenouchi: Fatigue of Nodal Joint, Box-section Truss Chords and Large Welded Joints, Colloquim IABSE, March 1982.
3) Matsuzaki, Y., H. Shimokawa and K. Murakami: Fatigue Design of Honshu-Shikoku Bridges in Japan, Colloquium IABSE, March 1982.
4) Tajima, J., A. Okukawa, M. Sugizaki and H. Takenouchi: Fatigue Tests of Panel Point Structures of Truss Made of 80 kg/mm² High Tensile Strength Steel. IIW No. 831–77, 1977.
5) Tajima, J., A. Okukawa and H. Takenouchi: Fatigue Tests of Panel Point Structures of Truss. Proceedings of 32th Annual Meeting of JSCE. I-326, 1977 (In Japanese).
6) Japan Society of Civil Engineers, Committee for Honshu-Shikoku Bridges: Design Guide for Panel Point Structures of Truss. 1976 (In Japanese).
7) Miki, C., F. Nishino, Y. Hirabayashi and H. Ohga: Fatigue Strength of Longitudinal Welded Joints Containing Blowholes. Proc. of JSCE. No. 325, pp. 155~165. 1982-9.
8) Hirt M. A., and J. W. Fisher: Fatigue Crack Growth in Welded Beams, Engineering Fracture Mechanics Vol. 5, pp. 415~429, 1973.
9) Miki, C., F. Nishino, J. Tajima and Y. Kishimoto: Initiation and Propagation of Fatigue Cracks in Partially-penetrated Longitudinal Welds, Proceeding of JSCE, No. 312, August 1981.
10) Miki, C., J. Tajima, K. Asahi and H. Takenouchi: Fatigue of Large-Sized Longitudinal Butt Welds with Partial Penetration. Proceeding of JSCE, No. 322, June 1982.
11) Miki, C., F. Nishino and Y. Hirabayashi: Fatigue Cracks Growth in the Corner Weld of Box-section Truss Chords, Colloquium IABSE, March 1982.

(Received December 16, 1982)

土木学会論文報告集　第341号

高張力鋼を用いたトラスの疲労強度

（田島二郎／竹名興英／三木千寿／伊藤文夫）

昭和59年1月

本州四国連絡橋の疲労設計に用いられる許容応力度は，1973年に土木学会本州四国連絡橋鋼上部構造研究委員会により，各種の継手構造に対する既存の疲労試験結果の 95％ 非破壊確率値に基づいて設定された．しかし今までに行われた疲労試験での試験体の形状や寸法は試験機の能力の制約から，かなり限られたものになっている．本州四国連絡橋の規模を考えると，寸法効果や構造部材としての二次的な応力の影響などを含めて，疲労許容応力度の適用性を確認する必要がある．その後，本州四国連絡橋公団では大型の継手試験体や構造物モデルに対する疲労試験を行い，1981年に疲労許容応力度の改訂をした．

本研究は高張力鋼を用いて製作されたトラスの疲労強度を調べることを目的としている．小型でしかも強度の高いトラス格点を得る目的で種々のディテールの格点構造を設計し，その概そ 1/4 の大きさの構造物モデルに対して疲労試験を行った．

試験体は5種類あり，それぞれ 600 MPa 級および 800 MPa 級の調質型高張力鋼を用いて製作されている．各型式試験体間の差は使用鋼材と斜材の取り付け方式にある．格点部を小さくする目的で，格点内の斜材ウェブの先端にダイアフラムを取り付けて，斜材の軸力を下弦材の上フランジに直接伝達するといったことを試みている．トラス弦材の角継手はレ形開先の部分溶込みであり，サブマージアーク溶接で施工されている．大部分の試験体の角溶接ルート部には，かなり大きい寸法のブローホールが発生している．

疲労試験は動的最大能力 4 MN の電気油圧型疲労試験機を用いて実施した．荷重波形は正弦波，載荷速度は 2.3 Hz である．トラス弦材に実際に作用している荷重の確認および格点部の応力分布性状を調べる目的で，疲労試験の前に静的載荷試験を行い，試験体各部のひずみを測定した．また，有限要素法による応力解析も行った．

トラス下弦材平行部では実測応力と計算応力は非常に良く一致している．トラス格点部内での主応力分布も実測値と解析値は良く一致している．下弦材のウェブ上縁ではガセットによる応力集中が生じており，ガセットのフィレット端部の実測応力は下弦材平行部のそれの 1.25～1.44倍となっており，その程度は斜材の軸力をガセットのみで伝達する継手型式の方が著しい．ガセットの下縁においても平行部に比べて 10％ 程度の応力上昇が認められる．

すべての試験体において，疲労試験は下弦材の角溶接部から発生した疲労きれつが伝播したことにより終了している．疲労試験終了後破面を露呈して調査した結果，大部分の疲労きれつは角溶接のルート部に存在したブローホールを起点としている．疲労きれつは下弦材平行部の角溶接部からの他に，ガセットのフィレット端部から発生している．その場合も疲労きれつの起点は角溶接ルート部のブローホールであるが，その寸法は平行部でのそれに比較してかなり小さく，前述のガセットによる応力集中の影響が明らかである．

本実験で得られた下弦材の公称応力範囲ときれつを発見したときの寿命の関係は，既存の縦方向溶接継手試験体の疲労試験結果に比べて著しく低く，実験値の大部分は前許容応力度を下回っており，半数は現行許容応力度をも下回っている．

破壊力学の手法を用いて下弦材角溶接部の疲労きれつ進展寿命を推定した．そのとき，溶接ルート部に存在するブローホールはその内接円を直径とする円板きれつに置換えている．推定寿命線は内接円の寸法を基準として分類した実験値と良く一致している．また角溶接部に対する現行許容応力度は初期欠陥を直径 2 mm とした推定寿命線とほぼ一致している．したがって，この許容応力度を適用する場合には直径 2 mm 以上のブローホールを防止しなければならない．ガセットのフィレット端部に隣接する角溶接部に対しては，ガセットによる応力集中の影響を考慮して，C等級の許容応力度を適用すべきである．その位置に 1 mm を超えるようなブローホールが完全に防止できる場合は部材平行部の角溶接部と同じB等級の許容応力が適用できる．